Spine Deformity (2024) 12:595–602
https://doi.org/10.1007/s43390-024-00833-y

BIOMECHANICS

Optimization of S2-alar-iliac screw (S2AI) fixation in adult spine deformity using a comprehensive genetic algorithm and finite element model personalized to patient geometry and bone mechanical properties

Ningxin Qiao[1,2] · Isabelle Villemure[1,2] · Zhi Wang[3,5] · Yvan Petit[4] · Carl-Eric Aubin[1,2,5]

Received: 16 November 2023 / Accepted: 20 January 2024 / Published online: 7 March 2024

Abstract

Purpose To optimize the biomechanical performance of S2AI screw fixation using a genetic algorithm (GA) and patient-specific finite element analysis integrating bone mechanical properties.

Methods Patient-specific pelvic finite element models (FEM), including one normal and one osteoporotic model, were created from bi-planar multi-energy X-rays (BMEXs). The genetic algorithm (GA) optimized screw parameters based on bone mass quality (BM method) while a comparative optimization method maximized the screw corridor radius (GEO method). Biomechanical performance was evaluated through simulations, comparing both methods using pullout and toggle tests.

Results The optimal screw trajectory using the BM method was more lateral and caudal with insertion angles ranging from 49° to 66° (sagittal plane) and 29° to 35° (transverse plane). In comparison, the GEO method had ranges of 44° to 54° and 24° to 30° respectively. Pullout forces (PF) using the BM method ranged from 5 to 18.4 kN, which were 2.4 times higher than the GEO method (2.1–7.7 kN). Toggle loading generated failure forces between 0.8 and 10.1 kN (BM method) and 0.9–2.9 kN (GEO method). The bone mass surrounding the screw representing the fitness score and PF of the osteoporotic case were correlated ($R^2 > 0.8$).

Conclusion Our study proposed a patient-specific FEM to optimize the S2AI screw size and trajectory using a robust BM approach with GA. This approach considers surgical constraints and consistently improves fixation performance.

Keywords Biomechanical performance · Genetic algorithm · Patient-specific finite element analysis · S2AI screw fixation

Introduction

Adults spine deformity (ASD) impacts 30% to 60% of older individuals with previously normal spinal curvature [1], and its prevalence is increasing with the aging population. ASD patients often experience diminished health-related quality of life and perform poorly on related parameters [2]. Instrumentation surgery, particularly with long instrumentation to the pelvis, is commonly employed to improve quality of life measures and prevent loosening and pseudarthrosis [3, 4]. When comparing S2-alar-iliac screws (S2AI) with traditional iliac screws, S2AI screws present a clear advantage due to their lower profile and reduced need for extensive dissections. These factors contribute to a decreased risk of complications and subsequent surgical interventions [5, 6]. However, modes of failure such as screw loosening, screw fracture, rod fracture, L5-S1 pseudoarthrosis, and kyphotic

✉ Carl-Eric Aubin
carl-eric.aubin@polymtl.ca

1 Institute of Biomedical Engineering, Polytechnique Montréal, PO Box 6079, Downtown station, Montreal, QC H3C 3A7, Canada

2 Sainte-Justine University Hospital Center, Montreal, Canada

3 Centre Hospitalier de l'Université de Montréal, Montreal, Canada

4 Department of Mechanical Engineering, Ecole de Technologie Supérieure, Montreal, Canada

5 Department of Surgery, Faculty of Medicine, Université de Montréal, Montreal, Canada

fracture of the sacrum are still observed [7–9]. Eastlack et al. found a higher rate of screw loosening with an odd ratio of 2.63 [10]. Especially in patients aged 70 years or older, the reported incidence of loosening ranges from 50 to 66% [11, 12]. Low bone mineral density particularly in severe osteoporosis cases among the elderly is a common cause of failed fusion [13, 14]. Age-related heterogeneity in pelvic bone density can further contribute to fractures, instrumentation failure, and overall pelvic strength and stability issues [15].

To reduce the risk of screw loosening, proper anchoring is essential [12]. Recent anatomical studies by Liu et al. [16] and Wu et al. [17] focused on optimizing the diameter and feasible insertion region for S2-alar-iliac (S2AI) screws. Liu et al. found an average maximum corridor radius of 6 mm in a study involving 40 individuals, while Wu et al. identified a wide range of feasible S2AI screw trajectories in the coronal and sagittal planes. Jeong et al. [18] fine-tuned the entry point for an 8.5 × 115 mm screw and recommended a medially offset entry point to ensure sufficient anchorage through the sacroiliac joint (SIJ). However, a significant limitation of these studies was the absence of biomechanical evaluation of screw fixation efficacy.

Finite element analysis (FEA) has been employed in recent studies to biomechanically analyze and optimize implants in various anatomical locations. A combination of design of experiments (DOE) and FEA has been used in numerous studies to enhance implant fixation strength [19–22]. However, the deterministic nature of this approach can lead to local optima and unnecessary complexity. To address these limitations, Caprara et al. [23] utilized a genetic algorithm (GA) with FEA to optimize the biomechanical performance of pedicle screws, resulting in a 26% increase in simulated pullout strength. However, the FEM was constructed from CT scans, which may pose challenges for clinical implementation. In clinical practice, standing bi-planar X-rays are the standard for medical exams, particularly in the context of scoliosis [24].

This study aims to optimize the biomechanical performance of S2AI screws using a GA optimization based on bone quality and FEA, with the potential to be applied in clinical practice.

Methods

Model setup

The patient-specific FEM setup described in previous works [20, 25] can be summarized as follows. CT scans of an osteoporotic 81-year-old female and a normal 35-year-old female from TCIA database [26] were used for simulation studies. Their CT scans were used to generate synthetic biplanar multi-energy X-rays (BMEXs) using a simulator provided by the manufacturer of the BMEX equipment to simulate routine clinical images. These BMEXs were marked with landmarks and used to identify their corresponding landmarks on the generic pelvic FEM with the purpose of obtaining the patient-specific 3D morphology. The pixel values on the BMEXs were used to estimate the volumetric bone mineral densities (vBMDs) of the trabecular bone, which were grouped based on value similarity and assigned to the patient-specific 3D morphology based on coordinate correspondence. Cortical bone densities were estimated based on age, with a 35% reduction for cases of osteoporosis and a 10% reduction for normal cases [27]. The patient-specific FEM included a layer of cortical bone surrounding the trabecular bone, with iliac thicknesses ranging from 0.3 to 5 mm and a sacral thickness of 1 mm [28]. Both the cortical and trabecular bones were represented using 3D 4-node tetrahedron elements with a characteristic length of 2 mm.

GA workflow

First, the variables to optimize were defined as the screw insertion point, the trajectory angles, and the screw size (Fig. 1). The screw insertion region was determined as a quadrilateral delimited by the line connecting the centers of the first and second foramens, 0.5 cm away from the first and second foramens, and 0.3 cm from the SIJ cartilage. This surface region was remeshed using 3-node triangular elements with a characteristic length of 1 mm, and each node was considered as a possible insertion point. Feasible trajectory angles with respect to sagittal (SA) and transverse (TA) planes were determined at 1° increments to cover all possible angles. Standard screws with diameters of 7.5, 8.5, or 9.5 mm and lengths of 80 or 100 mm were used. These screws were approximated as cylinders. Each solution was defined as a set of numerical values for each variable. Constraints were set to eliminate impractical solutions for screw insertion in the pelvis. These constraints included avoiding the critical external cortex of the iliac bone and ensuring that the screw passes through the SIJ cartilage. Solutions failing to meet these criteria were excluded.

A fitness score was assigned to each solution, indicating its ability to meet the desired criteria (Fig. 2). The score was calculated as the bone mass around the screw. This was based on elements within the walls of a hollow cylinder with a wall thickness equal to half of the major-minor diameter difference (Fig. 2a), as it was assumed that bone quality correlated with screw performance with the bone elements in the thread path undergoing the loads [29]. Another fitness function which sums the bone mass within the cylinder enclosing the entire screw was evaluated but not used in the GA to examine the potential impact of the fitness function definition on the results (Fig. 2b).

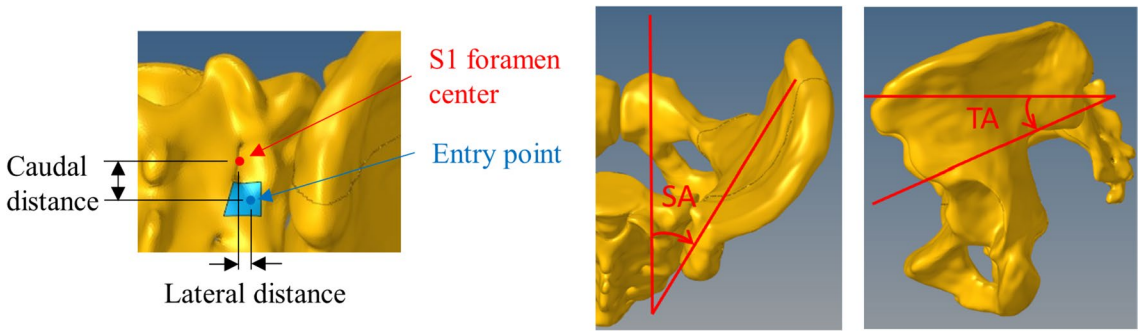

Fig. 1 Schematic representation of entry region (blue region) (left), trajectory angle with respect to the sagittal plane (SA) (middle), and trajectory angle with respect to transverse plane (TA) (right) for the right S2AI screw

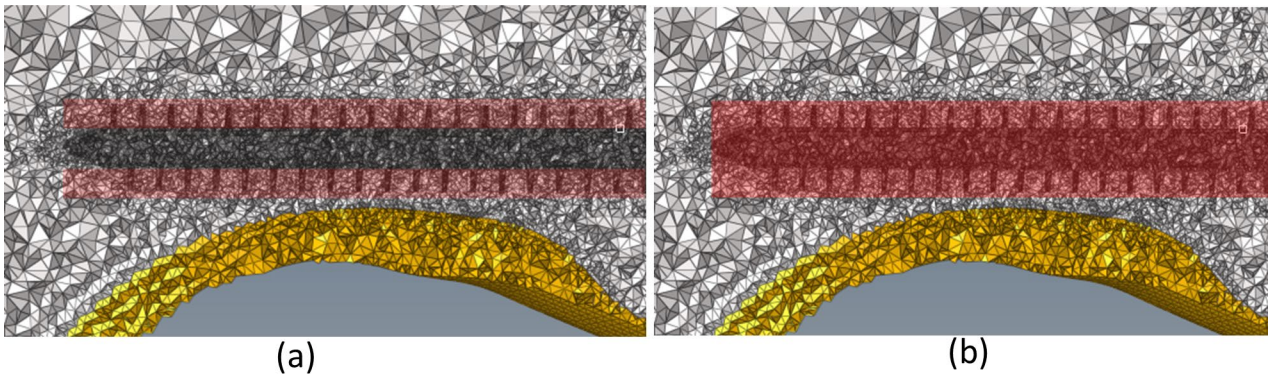

Fig. 2 Cross-section of **a** a hollow cylinder and **b** a full cylinder that were used to sum the properties in the red region to evaluate the fitness score. The trabecular bone is represented in white and the cortical bone in yellow

Ninety initial solutions were randomly generated and immediately checked for feasibility. We applied fitness-proportional selection to choose parent solutions from the current generation. We used a crossover operator with a 0.7 probability to generate two offspring solutions by exchanging variables. To ensure diversity, a mutation operator with a 0.2 probability was applied, randomly modifying one or more variables in each offspring. We repeated this process until the next generation had the same number of solutions, with old solutions being replaced by new ones. To preserve potentially valuable solutions, the five best solutions from the previous generation were retained. Finally, the program terminated after a fixed number of 35 generations.

To compare our method, referred to as BM in the subsequent section, with the approach of Liu et al. [16], referred to as GEO, we replicated their conditions. We established the entry point at the intersection of the median line between the upper and lower dorsal foramina and the lateral sacral crest line. Using a GA algorithm with the same parameters, workflow, and constraints as previously described, we derived the corresponding trajectory based on their criteria. We included three input variables: trajectory angles with respect to sagittal and transverse planes, as defined earlier, and the radius ranging from 0 to 15 mm in increments of 0.01 mm. The fitness value was set to the radius of the solution, enabling to determine the maximum inscribed cylinder centered at the typical entry point that permits the passage of the S2AI screw.

Finite element modeling and static load simulations on S2AI screws

The surface reconstruction of the patient-specific FEM was imported into Solidworks 2021 (Dassault Systèmes, Vélizy-Villacoublay, France). Next, the entry point and axis of the trajectory for each screw alignment as previously determined was defined. Bone elements along the screw were subtracted and the bone-screw elements were remeshed with 4-node tetrahedrons using HyperMesh 2020. The mesh surrounding the screw was fine-tuned to match the implant element size of 0.4 mm, while other areas were set to 1 mm to decrease computational time [20].

The bone material properties were then reassigned as described in our earlier work [25], as detailed in the Model

setup section. The ligament modeling was based on anatomical descriptions and utilized a viscoelastic generalized Kelvin–Voigt material law developed through an in-house experimental study [30]. The interosseous ligament was meshed using 3D 4-node tetrahedrons, while the anterior and posterior ligaments were meshed using 2D 3-node triangular shell elements. A summary of the material properties of the soft tissues can be found in Table 1.

The screw was considered as a rigid body due to its Young's modulus being significantly higher than those of the cortical and cancellous bones [20]. The bone-screw interface was modeled using a point-surface penalty method with Coulomb-type friction of 0.2 and a minimal gap of 0.05 mm, which has been previously validated [20, 22, 28]. The outer nodes of the ilium were fixed to create a stable support and the sacrum was allowed to move to simulate the natural movement of the pelvis.

Screw pullout was simulated, in addition to two toggle loading conditions in flexion with cephalad displacement and extension with caudal displacement on the screw head (Fig. 3), representing possible typical forces experienced by screws during daily activities. A constant displacement rate of 0.002 mm/min was applied to the screw head for all loadings until bone failure occurred. To prevent off-axis displacement, a constraining slide link condition was used, with only the screw axis translation free in the load direction. The resulting force–displacement (F-D) curves were used to calculate the initial stiffness (IS) and force to failure (FtF), characterized by a drop in the F-D curve [25]. Finally, we used a paired t-test to compare the FtF and IS of the best trajectories obtained from both the BM and GEO approaches.

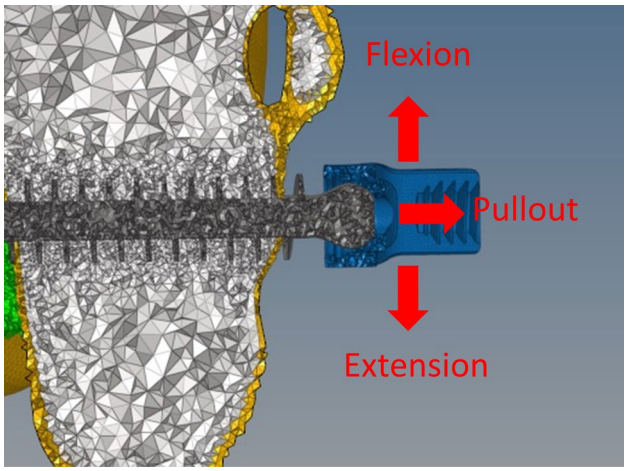

Fig. 3 Tested loadings applied to the screw head

Results

The optimal trajectories and their corresponding screw insertion inputs for each of the tested methodologies on both the left and right ilia of both osteoporotic and normal cases are presented in Table 2. Irrespective of the methodology or cases examined, the BM method consistently yielded higher fitness scores, insertion angles (SA and TA), and percentages of cortical bone mass compared to the GEO method. Furthermore, the largest screw sizes (9.5×80 mm, 9.5×100 mm, and 8.5×100 mm) consistently led to the optimal solutions regardless of the chosen method. Table 3 showcases five alternative solutions obtained using the BM method for the osteoporotic right ilium with only smaller screws (7.5×80 mm, 7.5×100 mm, and 8.5×80 mm) to illustrate the versatility of GA in generating multiple potential solutions based on predefined criteria.

The simulated pullout and toggling condition results for each trajectory in Table 2 are presented in Table 4. The BM method demonstrated higher FtF and IS values for pullout and extension conditions, while no significant differences were observed between the methods for flexion in terms of FtF and IS. In fact, There was a significant difference between the BM and GEO optimization methods in extension ($p < 0.05$) (Table 5). Within-pair correlations of the different loading conditions are either of the same level or higher for FtF compared to IS.

Finally, the coefficient of determination for the bone mass around the screw threads and the FtF was 0.84, and for the bone mass and the FtF was 0.87 (Fig. 4).

Table 1 Material properties of soft tissues

	Interosseous ligaments	Anterior ligaments	Posterior ligaments	Sacro-iliac joint (SIJ) cartilage
Young's modulus (MPa)	25	45	400	0.75
Poisson's ratio	0.3	0.3	0.3	0.4
Tangent Young's modulus (MPa)	10	10	100	–
Tangent Poisson's ratio	0.37	0.37	0.37	–
Viscoelastic constant	28	28	28	–
Navier constant	1.0^5	1.0^5	1.0^5	–

Table 2 Optimal trajectories (L = left ilium; R = right ilium)

		Optimization method	Screw size (mm)	SA (°)	TA (°)	Entry point (cm)[1]	Fitness score (g)	Cortical bone mass (%)
Osteoporotic case	L	BM	9.5 × 100	49	29	(1.1, 0.4)	3.0	60.6
		GEO	8.5 × 100	44	24	(1.5, 0.4)	1.7	43.0
	R	BM	9.5 × 100	53	30	(1.8, 0.0)	3.6	68.7
		GEO	9.5 × 100	49	30	(1.5, 0.4)	2.5	48.2
Normal case	L	BM	9.5 × 80	66	32	(1.4, 0.6)	4.0	80.4
		GEO	9.5 × 100	54	24	(1.4, 0.7)	2.5	47.1
	R	BM	9.5 × 100	60	35	(1.7, 0.0)	4.2	68.1
		GEO	9.5 × 100	44	30	(1.4, 0.2)	3.1	53.4

[1](Caudal, lateral) distance from S1 foramen

Table 3 Other optimal trajectories with smaller screws for the osteoporotic right ilium obtained using the BM method

Screw size (mm)	SA (°)	TA (°)	Entry point (cm)*	Fitness (g)	Cortical bone mass (%)
7.5 × 80	49	34	(1.8, 0.6)	2.2	81.2
7.5 × 80	54	34	(1.5, 0.0)	2.1	81.0
7.5 × 100	54	31	(1.8, -0.1)	2.6	77.8
7.5 × 100	55	36	(1.3, 0.1)	2.6	78.7
8.5 × 80	50	31	(2.0, 0.3)	2.7	79.5

*(caudal, lateral) distance from S1 foramen

Table 4 Results of Force to failure (FtF) and Initial stiffness (IS) for the simulated loading conditions of the trajectories in Table 2 (L = left ilium; R = right ilium)

		Optimization method	Pullout		Flexion		Extension	
			FtF (N)	IS (kN/mm)	FtF (N)	IS (kN/mm)	FtF (N)	IS (kN/mm)
Osteoporotic case	L	BM	4998	335.6	830	18.7	3148	195.2
		GEO	2076	94.3	888	19.2	1069	53.3
	R	BM	10,385	390.6	2118	64.1	4246	191.6
		GEO	5896	248.3	2049	41.8	1971	89.3
Normal case	L	BM	18,446	1322.7	3117	116.6	10,051	453
		GEO	5645	275.9	2932	53.9	2655	98.4
	R	BM	14,322	1182.1	2544	62.5	7365	332.3
		GEO	7690	302.3	2887	68.9	2610	153.4

Table 5 Statistical comparison between the BM and GEO optimization methods

		p-value	Within-pair correlation
FtF	Pullout	0.053	0.7
	Flexion	0.767	1.0
	Extension	0.046	0.9
IS	Pullout	0.084	0.7
	Flexion	0.301	0.6
	Extension	0.040	0.5

Discussion

In this study, a patient-specific FEM was used to optimize the S2AI screw fixation. Both BM and GEO optimization approaches favored the use of larger screws, which have been shown to achieve higher strength [22]. This is different from the goal of maximizing bone mineral density (BMD) around the screw tip [19]. Meanwhile, the BM approach with GA that maximizes total bone mass around screw improved FtF and IS compared to the GEO

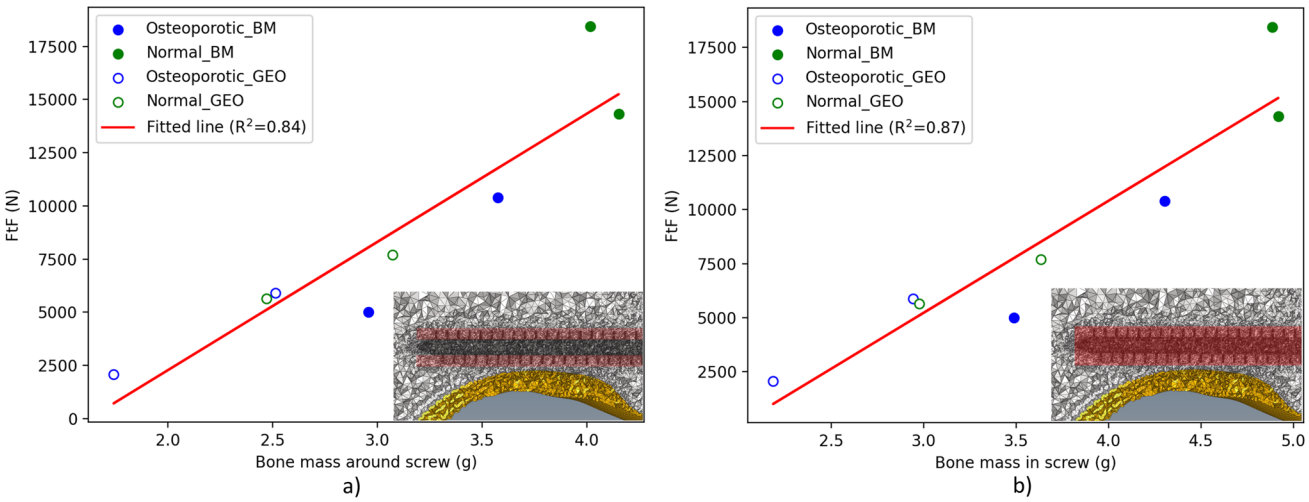

Fig. 4 Correlation between the fitness function (*x*-axis) and FtF (*y*-axis) for pullout test in osteoporotic and normal cases using BM and GEO optimization methods. The two fitness functions are: **a** the bone mass around the screw shank, and **b** the bone mass in the screw cylinder

approach, which maximizes the screw corridor radius [16]. This suggests that bone quality to be traversed is a more important feature than screw size for biomechanical performance, as shown by an R^2 value of 0.84 between bone mass around the screw and FtF (Fig. 4). In fact, the BM optimization consistently favored pelvic cortical bone crossing over the screw size, which provides better mechanical resistance to different loadings, although greater screw size was preferred in most cases as more bone could be involved in enhancing the bone-screw fixation. This is consistent with Caprara et al.'s study [23], which also favored a cortical bone trajectory, not consistently with the largest screw diameter. Therefore, our study supports the placement of the screw near the sciatic notch instead of the center of the tear drop, which was the initial approach in Luque Galveston and the subsequent first generation of iliac bolts [31].

The BM optimization approach resulted in screw entry points slightly more medially located compared to the standard insertion point, which aligns with findings from a recent cadaver study [18]. This medial placement allows for safer screw insertion into the sacrum and better alignment with long instrumentation. In contrast, the optimized trajectory using the GEO approach was more lateral and caudal, avoiding the anterior region of the great sciatic notch where nerves and arteries are present. Table 2 demonstrates a wide range of possibilities and variability in insertion angles, consistent with findings from anatomical studies [16]. The BM and GEO approaches differed by more than 5° in insertion angles in most cases, highlighting the clinical significance of this variation. The GEO approach yielded solutions closer to standard clinical practice [32], with a typical screw entry point located 10 mm laterally between the S1 and S2 foramina near the SIJ, and favoring a trajectory away from the pelvic cortex.

Local bone quality influenced the screw fixation in different functional loading conditions. The optimized trajectory from the BM method showed little improvement in all cases when applying flexion, in contrast to the optimized trajectory from the GEO method. This can be attributed to the fact that the screw moves in the cranial direction, where most of the bone material is trabecular. On the other hand, the extension simulations showed significant improvements due to the caudal location of the pelvic cortical wall relative to the screw placement. The pullout test that takes overall bone quality into account showed a significant improvement when using the BM method. Therefore, surgeons may want to consider using this method to maximize the bone quality around the screw and improve fixation strength.

Our study confirmed that various fitness functions have a strong positive correlation with biomechanical performance, as shown in Fig. 4. The correlation between the different fitness functions, namely the total bone mass around the screw shank (hollow cylinder) or the total bone mass in the screw cylinder (full cylinder), and the FtF consistently showed similar R^2 scores, as depicted in Fig. 4. This indicates that small variations in the bone mass included in the screw path are unlikely to significantly affect the predictive power of the model. While the method allows for the consideration of bone outside the threads and the exploration of different thread designs or screw shapes, it would need to be verified whether these factors would substantially enhance S2AI screw fixation.

Given the plausible range of viable solutions, the proposed optimization approach has several features that could be used for future surgery planning. Firstly, the BM

optimization method was developed based on BMEX technology, which could be used in the evaluation of ASD and surgical planning. The GA that was used in the BM method could be customized to a surgeon's technique or specified criteria, such as a pre-determined screw size as illustrated in Table 3. For patients with low bone quality who require risking cortical penetration for better fixation strength, which was the investigated scenario in this study, it is noteworthy that the optimized trajectory using the BM method in the osteoporotic case could achieve a similar level of strength as a more standard-like trajectory using the GEO method in the normal case, demonstrating the efficacy of the proposed BM method. Since the GA is versatile, a safety distance from the entire or specific region of the external cortical cortex could be added based on surgical considerations, to avoid cortical breach. Finally, the correlation observed between the BM and the pullout force (Fig. 4) provides surgeons with valuable information to evaluate the potential improvement in biomechanical performance by increasing the amount of BM around the screw. By increasing the amount of BM around the screw, surgeons can achieve greater cortical bone support without negatively impacting the biomechanical strength of the S2AI screws, which would occur if the cortex were breached [33]. Such information may help surgeons determine whether the potential benefits outweigh the associated risks.

There are a few limitations to this numerical approach. The biomechanical performance was based on three generic loading conditions, not necessarily representing all physiological loadings and the fatigue failure that the S2AI screw would undergo. However, this approach enables a consistent evaluation of the S2AI fixation performance after optimization using the BM method and direct comparison with reference cases, which are the trajectories from the GEO method. In addition, by analyzing the stress–strain behavior of the fixation during quasi-static loading, it is possible to estimate its fatigue behavior and potential risk of failure. Also, this study presents a comparative approach aimed at optimizing screw fixation in relative terms between the solutions tested, rather than precisely assessing stresses for implant design. Even if the sample size was small, the statistical significance was assured due to the high within-pair correlation [34], especially for FtF. Despite the limitations, this study suggests a workflow to biomechanically optimize S2AI fixation based on patient imaging data and highlights the practicality of using this approach to improve preoperative planning.

Conclusion

In this study, we proposed an original comprehensive patient-specific FEM to statistically optimize the S2AI trajectory. The optimized screw placement using the GA outperformed the reference optimization method based solely on the geometry, resulting in improved biomechanical performance and resistance to screw loosening in S2AI screw fixation. This approach enables identification of the best input parameters specific to each patient, while taking into consideration surgical constraints. The trajectories that were identified as the best from a purely biomechanical perspective consistently favored increased cortical bone around the screw while avoiding any breach of the cortex, significantly improving the biomechanical performance of the fixation, and the optimized trajectory could achieve the desired strength to resist screw loosening. The developed workflow for the pelvic fixation optimization suggests potential benefits for improving preoperative planning of spinopelvic fixation.

Acknowledgements The authors would like to thank Christian Bellefleur, Sophie Labat and Sajjad Rastegar-Talzali for their continuous support.

Author contributions Ningxin Qiao: Design, simulations, analysis, interpretation of the data for the work, drafting work, revising, final approbation, agree to be accountable. Isabelle Villemure: Design, interpretation of the data for the work, comprehensive review, final approbation, agree to be accountable. Zhi Wang: Interpretation of the data for the work, revising, final approbation, agree to be accountable. Yvan Petit: Interpretation of the data for the work, revising, final approbation, agree to be accountable. Carl-Eric Aubin: Design, interpretation of the data for the work, comprehensive review, final approbation, agree to be accountable.

Funding The project was funded by the Natural Sciences and Engineering Research Council of Canada (Industrial Research Chair program with Medtronic of Canada (IRCPJ 346145-16), and the Collaborative Research and Training Experience program).

Data availability The numerical data supporting the results of this study are available from the corresponding author upon reasonable request.

Declarations

Competing interests The authors disclose academic R&D support from Medtronic (Natural Sciences and Engineering Research Council of Canada (NSERC) industrial research chair program with Medtronic of Canada) and the NSERC-CREATE program.

References

1. Adrian K, Aftab Y, Patrick L (2020) Adult degenerative scoliosis—a literature review. Interdiscipl Neurosurg 20:100661
2. Diebo BG, Shah NV, Boachie-Adjei O et al (2019) Adult spinal deformity. Lancet 394:160–172
3. Moshirfar A, Rand FF, Sponseller PD, et al. (2005) Pelvic fixation in spine surgery. Historical overview, indications, biomechanical relevance, and current techniques. J Bone Joint Surg Am 87(Suppl 2):89–106
4. Yang H, Pan A, Hai Y et al (2023) Biomechanical evaluation of multiple pelvic screws and multirod construct for the

augmentation of lumbosacral junction in long spinal fusion surgery. Front Bioeng Biotechnol 11:1148342
5. Nanda A, Manghwani J, Kluger PJ (2020) Sacropelvic fixation techniques—current update. J Clin Orthop Trauma 11:853–862
6. Keorochana G, Arirachakaran A, Setrkraising K et al (2019) Comparison of complications and revisions after sacral 2 alar iliac screw and iliac screw fixation for sacropelvic fixation in pediatric and adult populations: systematic review and meta-analysis. World Neurosurg 132(408–20):e1
7. Guler UO, Cetin E, Yaman O et al (2015) Sacropelvic fixation in adult spinal deformity (ASD); a very high rate of mechanical failure. Eur Spine J 24:1085–1091
8. Martin CT, Holton KJ, Elder BD et al (2023) Catastrophic acute failure of pelvic fixation in adult spinal deformity requiring revision surgery: a multicenter review of incidence, failure mechanisms, and risk factors. J Neurosurg Spine 38:98–106
9. Martin CT, Polly DW, Holton KJ et al (2022) Acute failure of S2-alar-iliac screw pelvic fixation in adult spinal deformity: novel failure mechanism, case series, and review of the literature. J Neurosurg Spine 36:53–61
10. Eastlack RK, Soroceanu A, Mundis GM, Jr., et al. (2022) Rates of loosening, failure, and revision of iliac fixation in adult deformity surgery. Spine (Phila Pa 1976) 47:986–94
11. Iijima Y, Kotani T, Sakuma T et al (2020) Risk factors for loosening of S2 alar iliac screw: surgical outcomes of adult spinal deformity. Asian Spine J 14:864–871
12. Nakashima H, Kanemura T, Satake K et al (2020) The prevalence and risk factors for S2 Alar-Iliac screw loosening with a minimum 2-year follow-up. Asian Spine J 14:177–184
13. Tateen A, Bogert J, Koller H, et al. (2018) Complications of the lumbosacral junction in adult deformity surgery: indications and technique for posterior and anterior revision surgery. Orthopade 47:320–329
14. Krishnan V, Varghese V, Kumar GS et al (2020) Identification of pedicle screw pullout load paths for osteoporotic vertebrae. Asian Spine J 14:273–279
15. Inagaki N, Tanaka T, Udaka J et al (2022) Distribution of Hounsfield unit values in the pelvic bones: a comparison between young men and women with traumatic fractures and older men and women with fragility fractures: a retrospective cohort study. BMC Musculoskelet Disord 23:305
16. Liu F, Yang Y, Wen C et al (2020) Morphometric measurement and applicable feature analysis of sacral alar-iliac screw fixation using forward engineering. Arch Orthop Trauma Surg 140:177–186
17. Wu AM, Chi YL, Ni WF et al (2016) The feasibility and radiological features of sacral alar iliac fixation in an adult population: a 3D imaging study. PeerJ 4:e1587
18. Jeong ST, Park YS, Jung GH (2019) Computational simulation of sacral-alar-iliac (S2AI) screw fixation of pelvis and implications for fluoroscopic procedure: a cadaver study. J Orthop Surg (Hong Kong) 27:2309499019836246
19. Dominic M, Markus W, Boyko G et al (2020) Computational optimisation of screw orientations for improved locking plate fixation of proximal humerus fractures. J Orthopaed Transl 25:96–104
20. Fradet L, Bianco RJ, Tatsumi R et al (2020) Biomechanical comparison of sacral and transarticular sacroiliac screw fixation. Spine Deform 8:853–862
21. Bianco RJ, Arnoux PJ, Mac-Thiong JM et al (2019) Thoracic pedicle screw fixation under axial and perpendicular loadings: a comprehensive numerical analysis. Clin Biomech (Bristol, Avon) 68:190–196
22. Bianco RJ, Arnoux PJ, Wagnac E et al (2017) Minimizing pedicle screw pullout risks: a detailed biomechanical analysis of screw design and placement. Clin Spine Surg 30:E226–E232
23. Caprara S, Fasser MR, Spirig JM et al (2022) Bone density optimized pedicle screw instrumentation improves screw pull-out force in lumbar vertebrae. Comput Methods Biomech Biomed Eng 25:464–474
24. Graham RB, Sugrue PA, Koski TR (2016) Adult degenerative scoliosis. Clin Spine Surg 29:95–107
25. Qiao N, Villemure I, Aubin CE (2023) A novel method for assigning bone material properties to a comprehensive patient-specific pelvic finite element model using biplanar multi-energy radiographs. Comput Methods Biomech Biomed Eng. https://doi.org/10.1080/10255842.2023.2280764
26. Yorke AA, McDonald GC, Solis D, et al. (2019) Pelvic reference data: The Cancer Imaging Archive
27. Riggs BL, Wahner HW, Dunn WL et al (1981) Differential changes in bone mineral density of the appendicular and axial skeleton with aging: relationship to spinal osteoporosis. J Clin Invest 67:328–335
28. Dube-Cyr R, Villemure I, Arnoux PJ, et al. (2021) Instrumentation of the sacroiliac joint with cylindrical threaded implants: a detailed finite element study of patient characteristics affecting fixation performance. J Orthop Res 39(12):2693–2702
29. Joffre T, Isaksson P, Procter P et al (2017) Trabecular deformations during screw pull-out: a micro-CT study of lapine bone. Biomech Model Mechanobiol 16:1349–1359
30. Dube-Cyr R, Aubin CE, Villemure I et al (2020) Biomechanical analysis of two insertion sites for the fixation of the sacroiliac joint via an oblique lateral approach. Clin Biomech (Bristol, Avon) 74:118–123
31. Jain A, Hassanzadeh H, Strike SA et al (2015) Pelvic fixation in adult and pediatric spine surgery: historical perspective, indications, and techniques: AAOS exhibit selection. J Bone Joint Surg Am 97:1521–1528
32. Yilmaz E, Abdul-Jabbar A, Tawfik T et al (2018) S2 Alar-Iliac screw insertion: technical note with pictorial guide. World Neurosurg 113:e296–e301
33. O'Brien JR, Yu W, Kaufman BE, et al. (1976) Biomechanical evaluation of S2 alar-iliac screws: effect of length and quad-cortical purchase as compared with iliac fixation. Spine (Phila Pa) 2013;38:E1250–E1255
34. de Winter JCF (2013) Using the Student' s *t*-test with extremely small sample sizes